NONDETERMINISTIC ANALYSIS OF NONLINEAR STRUCTURES SUBJECTED TO EARTHQUAKE EXCITATIONS

by Joseph Penzien[I] and Shih-Chi Liu[II]

SYNOPSIS

A stationary, Gaussian, random process, having a prescribed non-uniform power spectral density function and consisting of 50 artificial earthquake accelerograms of short duration with intensity levels equivalent to the 1940 El Centro, California, earthquake, is generated on a digital computer. The response of numerous structural systems having various internal energy dissipation capabilities as characterized by nonlinear stiffness degrading and elasto-plastic models are determined for this process, and the extreme values of response are plotted in the form of probability distribution functions.

INTRODUCTION

For many years structural engineers have been concerned with the dynamic response of structural systems when subjected to strong motion earthquakes, and a great deal of insight into their behavior under these conditions has been obtained by theoretical studies based on deterministic methods. These methods have serious limitations, however, due to the fact that past recorded strong motion accelerograms, which are very limited in number, have been used to prescribe the ground motion inputs. Since seismic waves are usually initiated by irregular slippage along faults followed by numerous random reflections, refractions, and attenuations within the complex ground formations through which they pass, stochastic (or random) process representations of ground motion inputs should be more appropriate. The advantage of this type of representation is that the dynamic response of structural systems can be established in a probabilistic sense, thus providing a more rational basis for seismic resistant designs.

Unfortunately, due to the limited number of available strong motion accelerograms, it is extremely difficult to establish reliable stochastic models for ground motion by statistical means. For this reason, investigators have been forced to hypothesize stochastic models which are believed to possess the pertinent characteristics of real earthquakes and which can be correlated with existing strong motion data. Both stationary and non-stationary processes have been used for this purpose.(1-11)

To satisfy the requirements of the structural engineer, stochastic models of ground motion must properly reflect the damage potential of future earthquakes to a wide range of structural types. Valuable information regarding the performance of these structural types can be obtained directly from studies on the response characteristics of certain nonlinear single degree of freedom systems provided they possess appropriate dynamic properties. Therefore, the research investigation reported herein was

(I) Professor of Civil Engineering, University of California, Berkeley, California.

(II) Member of Technical Staff, Bell Telephone Laboratories, Whippany, N.J.

conducted with the following objectives in mind: (1) to develop a digital computer program for the generation of stochastic processes which possess the pertinent properties of strong ground motion as caused by earthquakes, (2) to establish the probabilistic maximum response of certain nonlinear single degree of freedom systems, including the ordinary elasto-plastic and stiffness degrading models to such processes, and (3) to compare and correlate the response of these nonlinear systems with their corresponding linear elastic systems, i.e., systems having the same corresponding initial stiffnesses and viscous damping ratios.

The stiffness degrading model referred to here was originally established by R. W. Clough[12] to represent the characteristic behavior of concrete frames as reported by N. Hansen and H. Conner[13].

STOCHASTIC MODEL OF GROUND MOTION

A. Type of Stochastic Model - Upon visual inspection of existing strong motion accelerograms, one is likely to conclude that any stochastic process representation of ground motion must be non-stationary. In the rigorous sense, this conclusion would be true; however, after careful consideration of (1) the lack of strong motion data for statistical studies, (2) the difficulties of establishing valid non-stationary characteristics, and (3) the ultimate objectives in choosing a model, this conclusion becomes debatable.

Most strong motion accelerograms recorded on firm alluvial soil contain a short phase (5-15 seconds) of relatively-stationary high-intensity oscillation having predominate frequencies in the range 2-5 cycles per second. Using these accelerograms as the prescribed excitation for structural systems, deterministic studies show that most of these systems experience their peak relative displacement response during this short phase[14]. Therefore, if peak relative response is being used to establish the degree of damage incurred, it seems reasonable to model only this short phase of the accelerograms using stationary processes of short duration.

Further, in support of this point of view, consider the non-stationary response of linear structural systems to stationary "white noise" excitation when "at rest" initial conditions are imposed. A non-deterministic solution of this problem shows that the ensemble mean square response of a typically damped system (5-10 percent of critical) approaches its stationary value in a very short period of time, i.e., within an interval corresponding to only a few periods of the fundamental mode of vibration[15]. Therefore, a stationary process of, say, 10 seconds duration for the excitation gives ample time for most linear buildings which have fundamental periods in the range 0-2 seconds to approach their steady state conditions. Thus, increasing the duration of excitation beyond this 10 second value has a relatively small effect on the probability distribution of peak response.

In view of this discussion, it seems reasonable to represent strong ground motion by short duration stationary processes when investigating the peak response of damped linear structures having fundamental periods

below approximately 2 seconds, and it is believed reasonable to also use this representation when investigating the peak response of certain elasto-plastic systems, provided there is no loss of strength associated with the inelastic deformations produced. In the latter case, stationary response levels are reached more slowly, therefore making it more important to select a realistic duration for the stationary process.

Due to the large number of random factors which influence the characteristics of strong motion accelerograms, one would expect, and indeed finds, that these wave forms are nearly Gaussian below the 3σ level (σ = standard deviation). Thus, a Gaussian distribution has been specified for the short duration stationary process used in this investigation.

B. Power Spectral Density Function - The power spectral density function for any stationary process which characterizes strong ground motion must, of course, reflect the correct frequency components within the real ground motion at any geographic location represented by the process. Since the local soil conditions greatly influence the characteristics of strong ground motion, the power spectral density function must be adjusted so as to be consistent with the soil conditions present.

To establish the form of the power spectral density function, one must rely upon time series analyses of existing strong motion records. Such analyses can be carried out by first evaluating the time average

$$\phi_a(\tau) \equiv \frac{1}{T_o} \int_0^{T_o} a(t)\, a(t+\tau)\, dt \qquad (1)$$

where $a(t)$ is the recorded ground acceleration, τ is a dummy time variable, and T_o is the duration of the record being analyzed, and then by taking the Fourier transform of $\Phi_a(\tau)$ using the relation

$$\theta_a(\omega) \equiv \frac{1}{2\pi} \int_{-\tau_o}^{\tau_o} \phi_a(\tau)\, e^{-i\omega\tau}\, d\tau \qquad (2)$$

where ω is a circular frequency and τ_o is a prescribed limit of integration based on convergence considerations. If the wave form being analyzed is stationary over an infinite duration, the functions $\Phi_a(\tau)$ and $\theta_a(\omega)$ approach the autocorrelation function $R_a(\tau)$ and power spectral density function $S_a(\omega)$, respectively, with increasing values of T_o and τ_o. Fortunately, convergence to the true functions takes place quite rapidly.

Appreciable variations are found in the functions $\Phi_a(\tau)$ and $\theta_a(\omega)$ for strong motion accelerograms even when representing similar soil conditions. Their general forms, however, have characteristics similar to those shown in Figs. 1b and 1c which were derived from the accelerogram (N-S component, El Centro, California, 1940) shown in Fig. 1a. It is of particular interest to note that the ordinates of the function $\theta_a(\omega)$ usually increase with increasing frequencies to a maximum value at some frequency which may be considered a characteristic ground frequency and then decreases rather rapidly towards zero in an asymptotic manner. This general rise and fall of the function is, however, accompanied by local random fluctuations.

Due to lack of statistical information, it is impossible to rigorously establish the form of power spectral density function $S_a(\omega)$ to be

used in the generation of short duration stationary processes which represent strong ground motions; however, if the intended use of these processes is primarily for investigating the general probabilistic features of peak structural response, it is believed that an averaged smooth version of functions $\theta_a(\omega)$ can be used for this purpose with reasonable success.

Extensive time series analyses of strong motion records have been conducted by K. Kanai and H. Tajimi which yielded results similar to those described above[16,17]. These investigators have suggested a power spectral density function of the form

$$S_a(\omega) = \frac{S_o\left[1 + 4\xi_g^2\left(\frac{\omega}{\omega_g}\right)^2\right]}{\left[1 - \left(\frac{\omega}{\omega_g}\right)^2\right]^2 + 4\xi_g^2\left(\frac{\omega}{\omega_g}\right)^2} \qquad (3)$$

where S_o is a constant power spectral density, ω_g is a characteristic ground frequency, and ξ_g is a characteristic damping ratio. Because of its simplicity and relative accuracy, the authors, as well as other investigators, have adopted this function for their investigations[4].

The fact that the function given by Eq. (3) does not reflect the local random fluctuations normally present in the function $\theta_a(\omega)$ merits some consideration, particularly if one is concerned with the peak response of narrow band systems to the prescribed random excitation. Due to the shortness in duration of real accelerograms, it is believed that such fluctuations will be generated by a time series analysis whether they are actually present or not. Therefore, any attempt to model such fluctuations does not appear justified at the present time.

It should be recognized that Eq. (3) represents the transfer function for a simple single degree of freedom system having a natural frequency ω_g and a viscous damping ratio ξ_g. In this case S_o represents a constant power spectral density function for acceleration at the support and $S_a(\omega)$ represents the power spectral density function for absolute or total acceleration of the system's lumped mass. Thus, for the case of surface ground acceleration, as represented by $S_a(\omega)$, S_o can be considered as a constant power spectral density function for acceleration at bedrock level, in which case the single degree of freedom transfer function represents the characteristics of the overlaying soil. Kanai has suggested 15.6 rads./sec. for ω_g and 0.6 for ξ_g as being representative of firm soil conditions. These numerical values were adopted by the authors in the investigation reported herein.

The variance σ_a^2 (or mean square value) of process a(t), as characterized by Eq. (3), is given by the relation[6],

$$\sigma_a^2 = \left[\left(\frac{1}{2\xi_g}\right) + 2\xi_g\right] \pi\omega_g S_o \qquad (4)$$

C. Generation of Stochastic Model - The procedure used to generate a Gaussian stationary process having a power spectral density function corresponding to Eq. (3) will now be described.

This procedure starts by sampling a sequence of pairs of statistically independent random numbers $x_1, x_2; x_3, x_4;$ --- $; x_{n-1}, x_n$, all of which have a

uniform probability distribution over the range $o < x < 1$. A new sequence of pairs of statistically independent random numbers y_1, y_2; y_3, y_4; --- ; y_{n-1}, y_n are then generated using the relations

$$Y_i = (-2 \log_e x_i)^{\frac{1}{2}} \cos 2\pi x_{i+1}$$
$$Y_{i+1} = (-2 \log_e x_i)^{\frac{1}{2}} \sin 2\pi x_{i+1} \qquad (5)$$

which have been shown to possess a Gaussian distribution with a mean of zero and a variance of unity[18-20].

A single wave form $y(t)$ can now be established by assigning the values $y_1, y_2, ---, y_n$ to n successive ordinates spaced at equal intervals $\Delta\varepsilon$ along a time abscissa and by assuming a linear variation of ordinates over each interval. Assume that the initial ordinate y_o, which is taken equal to zero, is located at $t = t_o$ where t_o is a random variable having a uniform probability density function of intensity $1/\Delta\varepsilon$ over the interval $o < t_o < \Delta\varepsilon$.

A complete ensemble of m such wave forms $y_r(t)$ $(r = 1,2,---,m)$ can be obtained by repeating this procedure m times, thereby creating an ergodic process which is completely characterized by the symmetric autocorrelation function

$$R_y(\tau) = \begin{cases} \frac{2}{3} - \left(\frac{\tau}{\Delta\varepsilon}\right)^2 + \frac{1}{2}\left(\frac{|\tau|}{\Delta\varepsilon}\right)^3 & -\Delta\varepsilon \le \tau \le \Delta\varepsilon \\ \frac{4}{3} - 2\left(\frac{|\tau|}{\Delta\varepsilon}\right) + \left(\frac{\tau}{\Delta\varepsilon}\right)^2 - \frac{1}{6}\left(\frac{|\tau|}{\Delta\varepsilon}\right)^3 & \begin{cases} -2\Delta\varepsilon \le \tau \le -\Delta\varepsilon \\ \Delta\varepsilon \le \tau \le 2\Delta\varepsilon \end{cases} \\ 0 & \tau \le -2\Delta\varepsilon;\ \tau \ge 2\Delta\varepsilon \end{cases} \qquad (6)$$

Suppose that the intensity of this process is now changed by multiplying each ordinate y_i in the process by the normalization factor $\sqrt{2\pi S_o/\Delta\varepsilon}$, where S_o is a constant. The autocorrelation function for the new process is obtained by simply multiplying the right hand side of Eq. (6) by $2\pi S_o/\Delta\varepsilon$, thus giving

$$R_y(\tau) = \begin{cases} \frac{2\pi S_o}{\Delta\varepsilon}\left[\frac{2}{3} - \left(\frac{\tau}{\Delta\varepsilon}\right)^2 + \frac{1}{2}\left(\frac{|\tau|}{\Delta\varepsilon}\right)^3\right] & -\Delta\varepsilon \le \tau \le \Delta\varepsilon \\ \frac{2\pi S_o}{\Delta\varepsilon}\left[\frac{4}{3} - 2\left(\frac{|\tau|}{\Delta\varepsilon}\right) + \left(\frac{\tau}{\Delta\varepsilon}\right)^2 - \frac{1}{6}\left(\frac{|\tau|}{\Delta\varepsilon}\right)^3\right] & \begin{cases} -2\Delta\varepsilon \le \tau \le -\Delta\varepsilon \\ \Delta\varepsilon \le \tau \le 2\Delta\varepsilon \end{cases} \\ 0 & \tau \le -2\Delta\varepsilon;\ \tau \ge 2\Delta\varepsilon \end{cases} \qquad (7)$$

It is significant to note that as $\Delta\varepsilon$ is allowed to approach zero, the autocorrelation function given by Eq. (7) approaches the relation

$$R_y(\tau) = 2\pi S_o \delta(\tau) \qquad (8)$$

where $\delta(\tau)$ is a Dirac delta function located at the origin $\tau = 0$. Therefore, in the limit this process becomes Gaussian "white noise" having a uniform power spectral density function of intensity S_o over the complete range of frequencies, i.e., over the range $-\infty < \omega < \infty$.

For practical reasons $\Delta\varepsilon$ must be taken as a finite quantity, but sufficiently small so that the resulting power spectral density function is nearly constant at intensity S_o over the lower range of frequencies (0-10 cps) which must be properly represented in the process. A value of 0.025 seconds was chosen for $\Delta\varepsilon$ in this investigation.

To establish the desired stationary process a(t), each member $y_r(t)$ (r = 1,2,---,m) of the normalized process y(t) must be filtered in accordance with Eq. (3). This step can be accomplished by assuming that a simple single degree of freedom system having an undamped circular frequency ω_g and a damping ratio ξ_g is subjected separately to the m support acceleration functions $y_r(t)$ and by calculating the corresponding absolute or total acceleration functions $a_r(t)$ of the mass. Mathematically, this statement is equivalent to saying that one must solve the differential equations

$$\ddot{z}_r(t) + 2\omega_g\xi_g\dot{z}_r(t) + \omega_g^2 z_r(t) = -y_r(t) \qquad r=1,2, ---, m \quad (9)$$

using appropriate random initial conditions to insure that z(t) is stationary and then evaluate the desired family of acceleration functions $a_r(t)$ using the relation

$$a_r(t) \equiv \ddot{z}_r(t) + y_r(t) \qquad r=1,2, ---, m \quad (10)$$

In this investigation, Eqs. (9) were solved numerically on a digital computer using a constant integration interval of 0.01 seconds and a procedure corresponding to the standard linear acceleration method(21).

D. Discussion of Standard Stochastic Model - A total of fifty artificial accelerograms (m = 50) were generated for process a(t) with a duration of 30 seconds which corresponds to $\Delta\varepsilon = 0.025$ seconds and n = 1200. The standard intensity S_o of the unfiltered "white noise" was set at 0.00614 $ft.^2/sec.^3$ so that the mean velocity response spectrum curves for the filtered process a(t) would give a "best fit" with the standard response spectrum curves published by G. Housner(22). This intensity is slightly less than the value of 0.0063 $ft.^2/sec.^3$ used by J. Penzien in a previous investigation to correlate the mean velocity response spectrum curves for "white noise" with Housner's standard curves(6).

The first two of fifty artificial accelerograms generated are shown in Figs. 2a and 2b. It is interesting to note that these accelerograms are very similar in appearance to the two real accelerograms presented in Figs. 2c and 2d except for the general stationary appearance of the artificial accelerograms.

The autocorrelation and corresponding power spectral density functions (as approximated by $\Phi_a(\tau)$ and $\theta_a(\omega)$, respectively) for the first two artificial earthquakes generated are shown in Figs. 3a-3d. It is of particular significance to note that while the power spectral density functions show noticeable variations from one to another, their average for ten artificial earthquakes as shown in Fig. 3f is quite close to the prescribed function (Eq. 3).

Since the local random type fluctuations appearing in the individual power spectral density functions are nearly eliminated by this averaging procedure, it would appear that a duration of 30 seconds is insufficient to allow full convergence to the true function during a time series analysis; thus, the appearance of similar fluctuations in the function $\theta_a(\omega)$ (Eq. 2) for real earthquakes are most likely the result of similar duration effects. Therefore, it does not seem reasonable at this time to attempt the inclusion of these variations in a stochastic model representing

strong motion accelerograms.

The total area (variance of the process σ_a^2) under the averaged power spectral density function in Fig. 3f is somewhat less than the area under the prescribed function due to the manner in which the "white noise" process y(t) was digitized in preparation for the numerical integration of Eqs. (9). Process y(t) was originally created by spacing the random ordinates y_i at 0.025 second intervals and by assuming a linear variation over each interval. However, since the numerical integration used a 0.010 second interval, it was necessary to digitize the process y(t) accordingly. Thus, small portions of the wave forms $y_i(t)$ were cut off at every other point of slope change in the function. These slight changes in the wave forms somewhat reduce the variance of this particular process and thus have a similar effect on process a(t).

This same area discrepancy was also observed when the average mean square value, σ_a^2, of the digitized ordinates (at 0.01 second intervals) of process a(t) was found equal to 0.54 $ft.^2/sec.^4$, which is somewhat below the theoretical value of 0.61 as given by Eq. (4).

Ground acceleration processes having durations shorter than 30 seconds were also established for purposes of studying the influence of duration on structural response. These processes were formed by simply taking specified portions of the 30 second duration process.

The numerical values of 15.6 rads/sec for ω_g and 0.6 for ξ_g as selected for this investigation represent firm ground conditions. If different ground conditions are to be represented by the stochastic process a(t), these parameters should be adjusted to reflect the proper frequency distribution.

RESPONSE OF LINEAR SINGLE DEGREE OF FREEDOM SYSTEMS

Complete time histories of response of viscously damped linear single degree of freedom systems when subjected separately to support accelerations $a_r(t)$ (r-1,2,---,50) were established by deterministic methods, i.e., by standard numerical integration procedures. The peak or extreme value of response was noted in each case, thus providing ordinates for standard velocity response spectrum curves as shown in Figs. 4a and 4b for the first 2 members of ensemble a(t), respectively, for 4 different values of the damping ratio ξ. Significant variations in these curves are noted from one ensemble member to another, especially for the lower values of damping. These variations can be expected, however, due to the random phase relations present in process a(t).

To obtain a set of velocity response spectrum curves for the entire process a(t), the response spectrum curves for all 50 members of the ensemble were averaged to give the results shown in Fig. 4c. This averaging procedure greatly reduces the local fluctuations which appear in the spectrum curves for individual members of the input process. The larger the number of curves averaged, the greater the "smoothing" effect.

As previously pointed out, the intensity S_o of the unfiltered "white

noise" was set at 0.00614 ft^2/sec^3 so that the mean velocity response spectrum curves (Fig. 4c) for higher damping ratios would give a "best fit" with Housner's standard spectrum curves (Fig. 4d).

It is important to realize that the averaged response spectrum curves represent statistical means and that a variance of peak response exists about each mean value. To show the degree of variance expected, probability distribution functions for the extreme values of relative displacement response will be presented subsequently for four different single degree of freedom systems representing a short and a long period structure, each of which has been assigned a low and a high damping ratio.

RESPONSE OF NONLINEAR SINGLE DEGREE OF FREEDOM SYSTEMS

Complete time histories of relative displacement response x(t) of the ordinary elasto-plastic and the stiffness degrading models were established by standard numerical integration procedures when subjected separately to support accelerations a(t) corresponding to the recorded N-S component of acceleration of the 1940 El Centro, California, earthquake and to the fifty artificially generated ground accelerations $a_r(t)$ previously described, but normalized by a factor of 2.90^2 so that they would correspond to the intensity level of the N-S component of the 1940 El Centro earthquake ($S_o = 2.90^2 \times 0.00614 = 0.0515\ ft^2/sec^3$).(4)

The basic parameters of the nonlinear models, which are also common to the linear models, are shown in Fig. 5. In all cases T and ξ represent the period of vibration and the viscous damping ratio, respectively, in the initial elastic range. The static force-deflection relations for the elasto-plastic and stiffness degrading models are shown in Figs. 5b and 5c, respectively. The strength ratio B and ductility factor DF are defined for these models in accordance with the relations $B \equiv V_y/W$ and $DF \equiv |x(t)|_{max}/x_y$. It is significant to note that in addition to loss of stiffness following any yielding, the stiffness degrading model permits hysteresis loops to be formed even at very low amplitudes of oscillation. Therefore, this model dissipates more energy in the low amplitude ranges of response than does the equivalent elasto-plastic model.

In this investigation, the response of the elasto-plastic and stiffness degrading models were studied for two different periods, T = 0.3 and 2.7 seconds, and for two different damping ratios, ξ = 0.02 and 0.10; thus, a total of 8 different nonlinear models were considered. Strength ratios B were selected for these models on the basis that the yield resistance V_y would equal twice the design load as specified in Section 2313(d) of the 1967 Uniform Building Code(23) for moment resisting frames, i.e., $B = 2KC = (2)(0.67)(0.05)(T)^{-1/3}$.

Extreme values of relative displacement response $|x(t)|_{max}$ were determined for each of the 8 nonlinear models defined above when excited separately by the 50 members of process a(t) (corresponding to S_o = $0.0515\ ft^2/sec^3$). These values are presented in the form of probability distribution functions in the next section of this paper.

Probability distribution functions $\Phi(|x|_{max})$ for the extreme values of relative displacement response as defined by the relation

$$\Phi(X) \equiv Pr[|x|_{max} < X] \tag{11}$$

are presented in the form of Gumbel plots in Fig. 6 for the 8 non-linear models previously described when excited separately by each member of process a(t) ($S_o = 0.0515$ ft^2/sec^3). For comparison purposes, probability distribution functions are also presented for the 4 corresponding linear elastic models, i.e., models having the same corresponding initial stiffnesses and viscous damping ratios. These models are identified by the arabic numerals 1-12 in Fig. 6 and have the properties listed in Table I.

Two probability distribution functions are shown in Fig. 6 for each of the 12 structural models, namely a wavy line function which is a plot of the actual extreme values determined for process x(t) and a straight line function which is a theoretical distribution of the form (24,25)

$$\Phi(|x|_{max}) = \exp(-e^{-y}) \tag{12}$$

where y is a reduced extreme value defined by the relation

$$y \equiv \alpha(|x|_{max} - u) \tag{13}$$

Constants α and u appearing in Eq. (13) can be determined using the relations[24]

$$1/\alpha = \sigma_x/\sigma_y \; ; \; u = \bar{x} - (\bar{y}/\alpha) \tag{14}$$

where σ_x and $\bar{x}$ represent the standard deviation and mean value, respectively, for the 50 extreme values of x(t) and where σ_y and $\bar{y}$ represent the standard deviation and mean value, respectively for the reduced extreme values y. The numerical values of σ_y and $\bar{y}$ depend upon the number of observed extreme values. When this number equals 50, as in this investigation, $\sigma_y \equiv 1.1607$ and $\bar{y} = 0.5485$.[24] The numerical values for σ_x and $\bar{x}$ and the corresponding values for $1/\alpha$ and u are given in Table I for each of the 12 structural models studied.

The probability distribution scale on Gumbel extreme value charts as shown in Fig. 6 varies in such a manner that Eq. (12) plots as a straight line with its ordinate u at the origin (y = 0) representing the most probable extreme value and with its slope being proportional to the standard deviation of the extreme values. Note that the extreme values in Fig. 6 for the nonlinear models can be measured also in terms of the ductility factor and that the probability distribution can be measured in terms of the return period, i.e., the expected number of earthquakes required to produce a single extreme value having the magnitude shown by the ordinate scale.

The significant features to be noted in Figs. 6a and 6b are the following: (1) The most probable extreme values of response for short period structures as represented in Fig. 6a are much greater for the elasto-plastic and stiffness degrading models than for their corresponding linear models, are appreciably greater for the elasto-plastic models than for their corresponding stiffness degrading models, and are considerably

greater for those models having 2 percent of critical damping than for their corresponding models having 10 percent of critical damping. (2) The most probable extreme values of response for long period structures as represented in Fig. 6b are considerably greater for those models having 2 percent of critical damping than for their corresponding models having 10 percent of critical damping; however, these values differ very little from one model to another. (3) The standard deviations of extreme value response for the short period structures are considerably larger for the elasto-plastic and stiffness degrading models than for their corresponding linear models and are appreciably larger for the elasto-plastic models than for their corresponding stiffness degrading models. (4) The standard deviations of extreme value response for long period structures correlate in a manner quite similar to short period structures except that the differences are not so great. (5) Increasing the viscous damping ratio increases the standard deviations of extreme value response for each model type. (6) The theoretical straight line functions as represented by Eq. (12) show very good correlations with the actual distributions.

EFFECT OF DURATION ON PEAK RESPONSE

The probability distribution functions for peak response in Fig. 6 result from an input process a(t) having a duration of 30 seconds. To determine the influence of duration on peak response, a number of shorter duration processes were also used in the general investigation reported herein.

To illustrate these effects, a ratio of the ensemble average of extreme value response for a variable duration T_o, $E[x_{max}]$, T_o, to the ensemble average of extreme value response for a fixed duration of 30 seconds, $E[x_{max}]$, 30, is plotted in Fig. 7 as a function of the duration ratio $T_o/30$.

It is quite evident, based on Curve No. 2 in Fig. 7a, that the mean peak response of typically damped, linear, short period structures (T = 0.3 seconds) increases very slowly with duration beyond approximately 6 seconds. Long period structures are, of course, more sensitive to duration as shown by Curve No. 2 in Fig. 7b. This curve indicates that the magnitude of mean peak response for a 15-second duration process is approximately 95 percent of the magnitude observed for a 30-second duration process. As shown in Figs. 7a and 7b, elasto-plastic and stiffness degrading structures are much more sensitive to duration than are elastic structures; thus, it is apparent that realistic durations must be used for stationary inputs when investigating the response of nonlinear structures.

CONCLUDING REMARKS

As demonstrated in this paper, stationary processes of short duration can be used quite effectively to establish the probabilistic peak response of both linear and nonlinear structural systems to strong motion earthquakes of a given intensity level. In the future, however, when the true dynamic characteristics of real structures become better known, damage is likely to be measured using various accumulative damage criteria,

in which case it will become more important that appropriate nonstationary processes be developed for damage prediction studies.

ACKNOWLEDGMENTS

The authors wish to express their sincere appreciation to the National Science Foundation for its financial support of this investigation under Grant NSF-GK-1319. Thanks are also due John A. Blume and Associates for permitting Dr. Liu to complete the computer programming as an employee of that firm.

BIBLIOGRAPHY

1. Bycroft, G. N., "White Noise Representation of Earthquakes," Proceedings ASCE, EM2, April, 1960.

2. Rosenblueth, E., and Bustamente, J. I., "Distribution of Structural Response to Earthquakes," Proceedings, ASCE, EM3, June, 1962.

3. Caughey, T. K., and Gray, A. H., discussion of "Distribution of Structural Response to Earthquakes," by Rosenblueth, E. and Bustamente, J. I., Proceedings, ASCE, Vol. 89, EM2, April, 1963.

4. Housner, G. W., and Jennings, P. C., "Generation of Artificial Earthquakes," Proceedings, ASCE, Vol. 90, EM1, February 1964, pp. 113-150.

5. Thomas, W. T., "Spectral Aspect of Earthquakes," Bulletin of the Seismological Society of America, Vol. 49, January 1959, pp. 91-98.

6. Penzien, J., "Application of Random Vibration Theory in Earthquake Engineering," Bull. of the Int. Inst. of Seis. and Earthquake Eng., Vol. 2, 1965, pp. 47-69.

7. Bogdanoff, J. L., Goldberg, J. E., and Bernard, M. C., "Response of a Simple Structure to a Random Earthquake-Type Disturbance," Bulletin of the Seismological Society of America, Vol. 51, No. 2, April 1959, pp. 293-310.

8. Goldberg, J. E., Bogdanoff, J. L., and Sharpe, D. R., "The Response of Simple Nonlinear Systems to a Random Disturbance of Earthquake Type," Bulletin of the Seismological Society of America, Vol. 54, No. 1, February 1964, pp. 263-276.

9. Amin, M. and Ang, H. H. S., "Nonstationary Stochastic Models of Earthquake Motions," Proceedings, ASCE, Vol. 94, No. EM2, April 1968, pp. 559-583.

10. Ward, H. S., "Analog Simulation of Earthquake Motions," Proceedings, ASCE, Vol. 91, EM5, October 1965.

11. Shinozuka, M., and Sato, Y., "Simulation of Nonstationary Random Process," Proceedings, ASCE, Vol. 93, No. EM1, February 1967, pp. 11-40.

12. Clough, R. W., "Effect of Stiffness Degradation on Earthquakes Ductility Requirements," Tech. Rep. No. 66-16, Struct. & Mat. Res., Dept. of Civil Engineering, University of California, Berkeley, October 1966.

13. Hanson, N. W., and Conner, H. W., "Reinforced Concrete Beam-Column Connections for Earthquakes," Prelim. Rep., Portland Cement Ass., November 1965.

14. Bogdanoff, J. L., "Comments on Seismic Accelerograms and Response Spectra," (Preliminary Report) Joint U. S. - Japanese Seminar in Applied Stochastics, NSF-JSPS, Tokyo, May 1966.

15. Caughey, T. K., "Transient Response of a Dynamic System Under Random Excitation," J. of Applied Mech., Trans. of the ASME, December 1961, pp. 563-566.

16. Kanai, K., "Semi-Empirical Formula for the Seismic Characteristics of the Ground," Bull. of the Earthquake Res. Inst., University of Tokyo, Japan, Vol. 35, June 1967, pp. 308-325.

17. Tajimi, H., "A Statistical Method of Determining the Maximum Response of a Building Structure During an Earthquake," Proceedings of the 2nd World Conference on Earthquake Engineering, Tokyo and Kyoto, Japan, Vol. II, July 1960.

18. Box, G. E. P., and Muller, M. E., "A Note on the Generation of Random Normal Deviates," Ann. Math. Statist., 34, 1963, pp. 1259-1264.

19. Franklin, J. N., "Deterministic Simulation of Random Processes," Mathematics of Computation, Vol. 17, No. 81, Jan. 1963, pp. 38-59.

20. Franklin, J. N., "Numerical Simulation of Stationary and Nonstationary Gaussian Random Processes," SIAM Review, Vol. 7, No. 1, January 1965.

21. Wilson, E. L., and Clough, R. W., "Dynamic Response by Step-by-Step Matrix Analysis," Paper No. 45, Sym. on the Use of Computers in Civil Engineering, Lisbon, Portugal, October 1-5, 1962.

22. Housner, G. W., "Design of Nuclear Power Reactors Against Earthquakes," Proceedings of the 2nd World Conference on Earthquake Engineering, Tokyo and Kyoto, Japan, Vol. I, July 1960.

23. Uniform Building Code, 1967 Edition.

24. Gumbel, E. J., "Statistical Theory of Extreme Values and Some Practical Applications," National Bureau of Standards Applied Mathematics Series, No. 33, February 12, 1954.

25. Gumbel, E. J., "Probability Tables for the Analysis of Extreme-Value Data," National Bureau of Standards Applied Mathematics Series, No. 22, July 6, 1953.

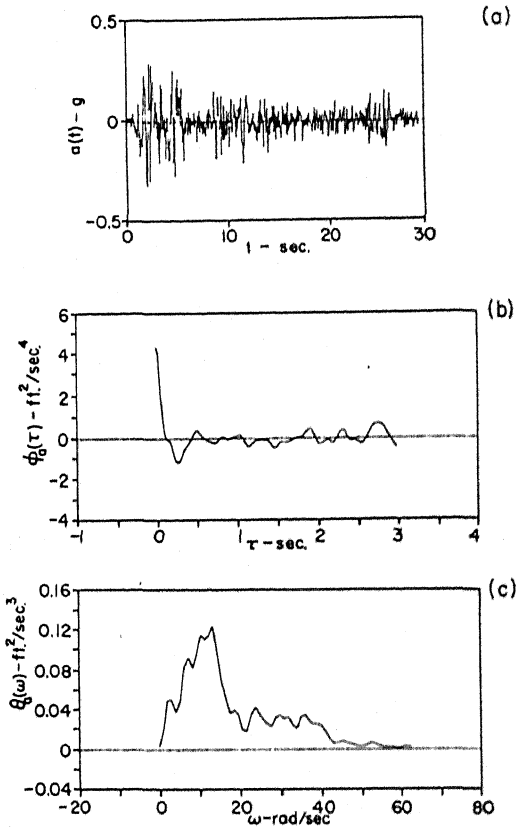

FIG. 1 ACCELEROGRAM a(t) AND FUNCTIONS $\phi_a(\tau)$ AND $\theta_a(\omega)$ FOR EL CENTRO, CALIFORNIA 1940, N-S COMPONENT

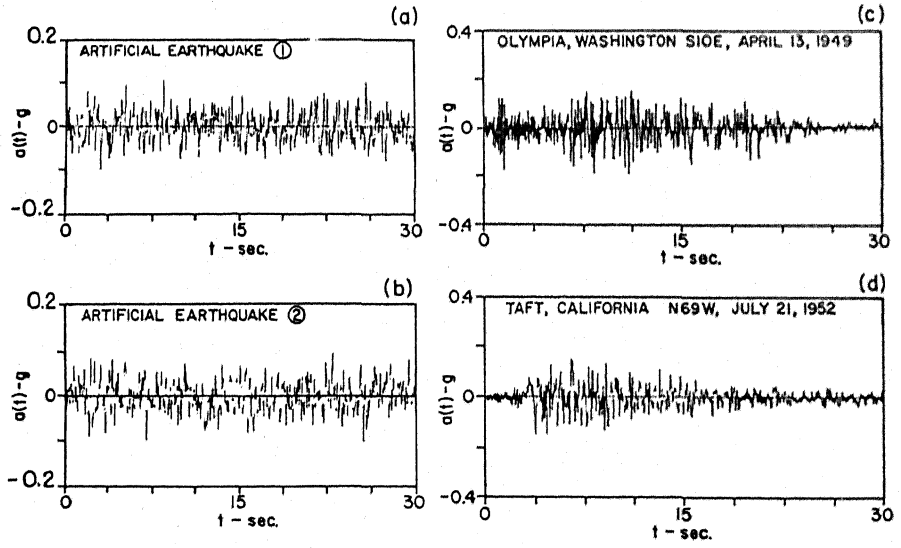

FIG. 2 GROUND MOTION ACCELEROGRAMS

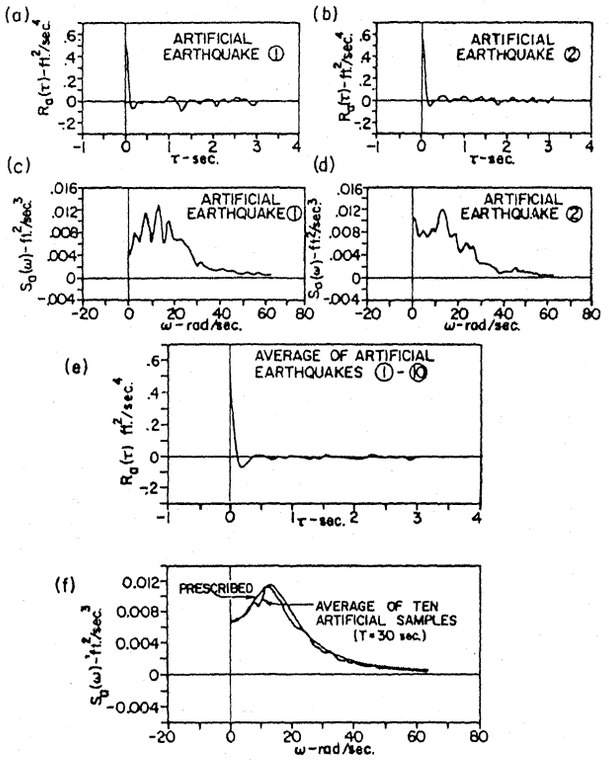

FIG. 3 AUTOCORRELATION AND POWER SPECTRAL DENSITY FUNCTIONS FOR ARTIFICIAL EARTHQUAKES.

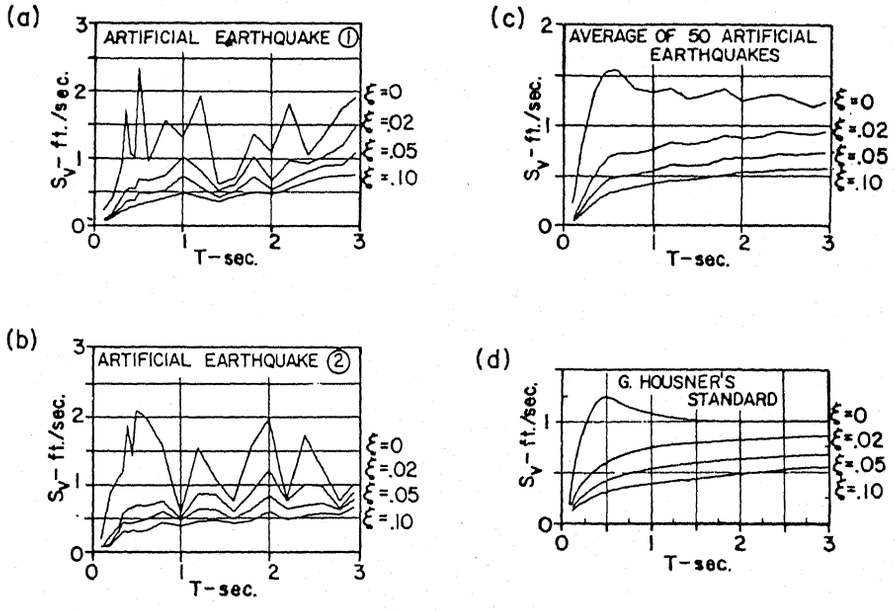

FIG. 4 VELOCITY SPECTRUM CURVES

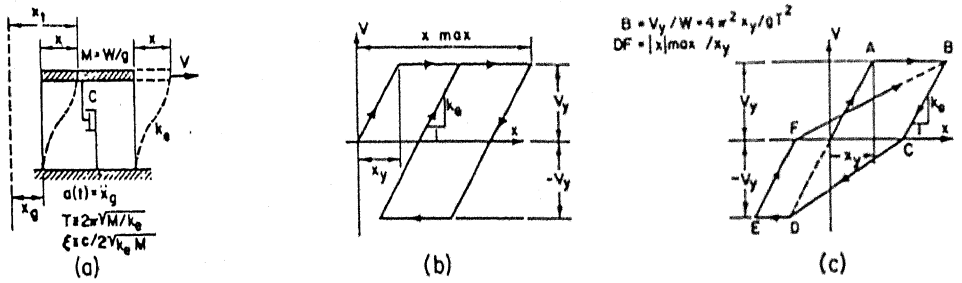

FIG. 5 NONLINEAR MODELS OF SINGLE DEGREE OF FREEDOM SYSTEM

TABLE I

CASE NO.	STRUCTURAL TYPE ψ	PERIOD T-SEC	DAMPING RATIO-E	STRENGTH RATIO-B	YIELD DISPL X - IN.	σ_x IN	$\bar{x}$ IN	u IN	I/Q
1	E	0.3	0.02	-	-	0.115	0.768	0.722	0.085
2	EP	0.3	0.02	0.10	0.088	1.613	3.214	2.450	1.390
3	SD	0.3	0.02	0.10	0.088	0.711	2.480	2.144	0.613
4	E	0.3	0.10	-	-	0.050	0.354	0.330	0.043
5	EP	0.3	0.10	0.10	0.088	0.910	1.947	1.517	0.784
6	SD	0.3	0.10	0.10	0.088	0.360	1.327	1.157	0.310
7	E	2.7	0.02	-	-	3.07	14.15	12.73	2.59
8	EP	2.7	0.02	0.048	3.42	5.51	16.35	13.75	4.75
9	SD	2.7	0.02	0.048	3.42	5.83	14.32	11.56	5.02
10	E	2.7	0.10	-	-	1.31	8.77	8.24	0.97
11	EP	2.7	0.10	0.048	3.42	4.56	11.57	9.41	3.94
12	SD	2.7	0.10	0.048	3.42	3.26	9.98	8.45	2.80

ψ E – ELASTIC
EP – ELASTO-PLASTIC
SD – STIFFNESS DEGRADING

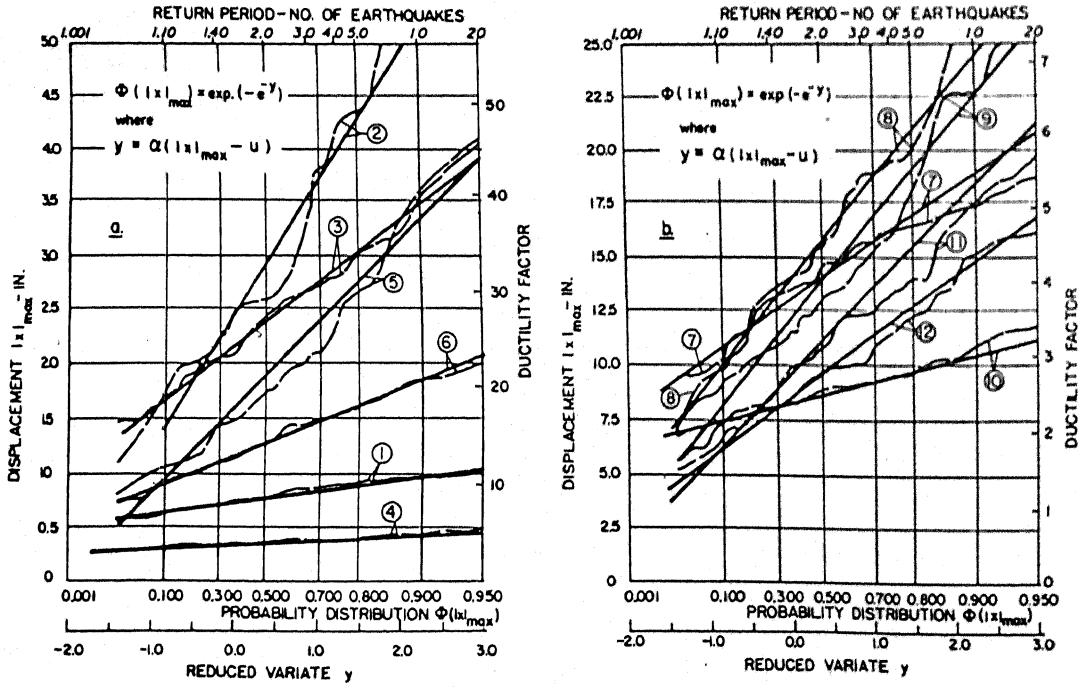

FIG. 6 PROBABILITY DISTRIBUTION FOR EXTREME VALUES OF RELATIVE DISPLACEMENT

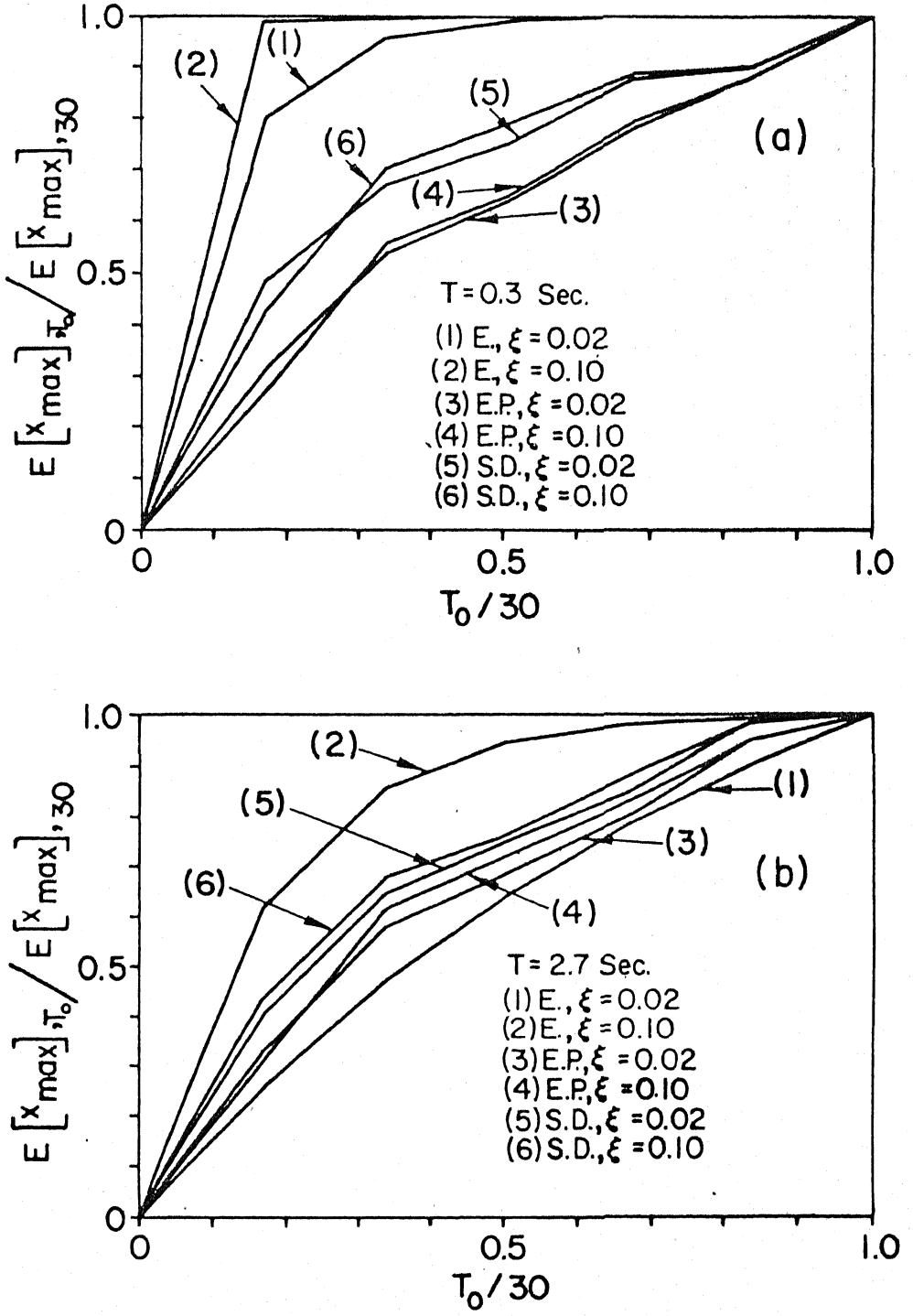

FIG. 7 DURATION EFFECT OF STATIONARY PROCESS ON MEAN PEAK RESPONSE OF LINEAR AND NONLINEAR STRUCTURES